LA-UR -84-635

CONF-840629--2

LA-UR--84-635

DE84 007466

TITLE: EFFICIENT FORWARD CONVERSION IN A RAMAN GENERATOR

AUTHOR(S): J. L. Carlsten, J. M. Telle, and R. G. Wenzel

SUBMITTED TO: Journal of Quantum Electronics

Los Alamos Los Alamos National Laboratory
Los Alamos, New Mexico 87545

EFFICIENT FORWARD CONVERSION IN A RAMAN GENERATOR

J. L. Carlsten, J. M. Telle, and R. G. Wenzel

Chemistry Division, Los Alamos National Laboratory
Los Alamos, New Mexico 87545

Abstract

Stimulated Raman scattering of an XeCl laser at 308 nm in a high pressure H_2 cell shows anomalously high conversion into first Stokes (S1) when a pumping geometry with a Fresnel number near unity is used. Specifically a quantum efficiency of 88% is obtained into S1. Comparison with a plane-wave model indicates that a theory including diffraction and 4-wave mixing may be necessary to understand the anomalous holdoff of the second Stokes component.

One of the most efficient methods for shifting a laser to longer wavelengths is by Stimulated Raman Scattering (SRS). The conversion efficiency is generally much higher for first Stokes (S1) generation when the gain for the second Stokes (S2) wave is considerably lower allowing S1 to grow without competition from S2. For example in SRS of visible or uv lasers in metal vapors, generally a system can be chosen where the scattering to S1 is more resonant than for S2, leading to quantum efficiencies as high as 70-80%.[1,2] If the S2 frequency is considerably lower than S1, as is the case of rotational SRS of infrared lasers, large quantum efficiencies of S1 can also been seen[3,4] when optical losses are folded out. This is because the gain for Stokes generation decreases with Stokes wavelength and hence the gain for S2 is considerably lower.

However for scattering of visible and uv lasers in gases such as H_2 or CH_4, the gain for S2 generation is not substantially lower than that for S1 since the Raman shift is small compared to the laser frequency and the laser frequency is far from being near the lowest electronic resonances which generally lie in the region of 80,000 - 100,000 cm^{-1} above the ground state. In addition at low pressures 4-wave mixing of the pump and S1 can produce S2 which can "seed" the pure Raman scattering of S1 into S2, and limit the conversion efficiency into S1 still more. Hence even at high pressure, which minimizes the 4-wave mixing, the quantum efficiency for S1 is generally limited to ~50% due to the onset of S2 when one uses a simple single focus generator design.[5] The efficiency can be raised substantially by utilizing a generator-amplifier system[6] which attenuates the higher-order Stokes components before entering the amplifier and therefore enhances the S1 conversion. By utilizi[illegible] backward SRS one can raise the quantum efficiency to ~85%,[7] since 4-wav[illegible] mixing does not phase match for the counter-propagating waves. However for backward SRS the linewidth of the laser must be smaller than the Raman bandwidth, which is often a severe requirement on the laser.

In this letter we report on vibrational SRS on the $Q_{01}(1)$ transition using a XeCl laser at 308 nm. We have attempted to limit the S2 generation due to 4-wave mixing by operating at high pressures to reduce the coherence length for the 4-wave process and also by utilizing a pumping geometry with a Fresnel number close to unity to reduce the angles which also lead to phase matching for 4-wave mixing.

Initially it was expected that at high pressures where 4-wave mixing is small due to the short coherence length and at low angles where the beam is close to plane wave, that a model which neglects diffraction and 4-wave mixing would be sufficient. In this case the equations of motion for the pump intensity I_P, the first Stokes intensity I_{S1} and second Stokes intensity I_{S2} in steady state are given by:[8,9]

$$\frac{d}{dz} I_{S1} = \alpha_P I_P I_{S1} - \alpha_{S1} \frac{\omega_{S1}}{\omega_{S2}} I_{S2} I_{S1} \qquad (1)$$

$$\frac{d}{dz} I_{S2} = \alpha_{S1} I_{S1} I_{S2} \qquad (2)$$

$$\frac{d}{dz} I_P = - \alpha_P \frac{\omega_P}{\omega_{S1}} I_{S1} I_P \qquad (3)$$

where z is the distance of propagation through the cell, α_P and α_{S1} are the plane wave gain coefficients for scattering of P into S1 and S1 into S2,[9,10] respectively and the ω's are the frequencies of the pump and Stokes waves.

The experimental apparatus is shown in Fig. 1. A Lambda-Physik EMG 150 injection-locked XeCl laser at 308 nm was clipped by aperture A1 before being focused with a 2 m lens into the center of a 50 cm H_2 cell. The beam was then recollimated by L2 and separated into the various frequency components by a brewster-angle prism P1.

It was found that varying the size of the aperture A1 had a very dramatic effect upon the conversion efficiency of both S1 and S2. Figure 2 shows the variation in quantum efficiency as a function of aperture diameter when the fluence incident on the aperture was ~44 mJ/cm^2. The quantum efficiency was taken as the photon conversion efficiency with the low intensity transmission losses folded out. An inventory of the energy into and out of the cell balanced to within 5% when Fresnel reflection losses and the energy deposited in the gas were taken into account. As seen in Fig. 2, as the aperture diameter is increased, initially S1 rises rapidly to a maximum of ~88% near 4.5 mm and then falls as the diameter is increased further where S2 conversion becomes significant. One might suspect that the growth of S2 at large apertures is due solely to a larger amount of energy being transmitted by a larger aperture. However our experiments have shown that at larger apertures S2 generation is considerably more significant even if the beam is attenuated to the same energy incident on the cell.

We also found that as the pressure of the H_2 was lowered, the quantum efficiency of S1 dropped while the conversion to S2 and other higher order Stokes components increased.

Figure 3 shows the quantum efficiency vs pump energy incident on the Raman cell with 1430 psi of H_2 and with the aperture set to a diameter of 4.5 mm which corresponds to the peak for S1 conversion in Fig. 2. The solid lines show the expected growth of S1 and S2 by the plane-wave model given by eqs. 1-3. A predictor-corrector integration scheme was used in this calculation for the experimental pulse shape given in Fig. 4. The pump intensity was somewhat arbitrarily chosen to be the average intensity at one Rayleigh range away from focus where the Rayleigh range was calculated for a Gaussian beam with 3 ω_0 equal to the diameter 4.5 mm of aperture A1.

As can be seen in Fig. 3, the onset of S1 is predicted quite well by the model but the growth of S2 is much different than seen experimentally. The model (solid line) predicts that S2 should start to be significant at ~2 mJ, while experimentally S2 is just starting to be observable at ~8.5 mJ. The dashed curve shows what the model predicts when the gain for S2 is set to zero (α_{S1} = 0) which surprisingly fits quite well. The implication is that for some reason the S2 generation is somehow prevented by the pumping geometry.

Figure 4 shows the observed pump depletion for an aperture diameter of 4.5 mm and an incident pump energy of 6.5 mJ. The solid lines show the experimental input and output pulse. The input pulse shape was taken with the cell removed. Integration of these pulse shapes showed a pump depletion of 86% in close agreement with the quantum efficiency observed in Figs. 2 and 3. The dotted line shows the pump depletion predicted from eqs. 1-3 with the gain for S2 set to zero. The agreement of the threshold is quite good but the experimental depletion is not as substantial as predicted by the plane wave model. We believe this is due to the low conversion in the low-intensity spatial wings of the pump beam at focus.

In conclusion we have substantially reduced the production of second Stokes (S2) generation and hence enhanced the first Stokes ( ) generation in a high pressure Raman cell with a low angle beam. Quantum efficiencies as high as 88% have been observed for S1. The threshold for the growth of the S1 component is found to be accurately predicted by a plane-wave model. However, the onset of S2 is not observed to occur where predicted by the simple plane-wave model which also neglects 4-wave mixing as a source term for S2 generation. We conclude that both diffraction and 4-wave mixing may be important in developing an understanding of these unexpected results.

The authors would like to thank J. R. Ackerhalt, I. J. Bigio, K. Druhl, R. A. Fisher, and N. A. Kurnit for numerous discussions about these results. The authors would also like to thank D. L. Barker and M. E. Weber for their excellent technical help on this experiment.

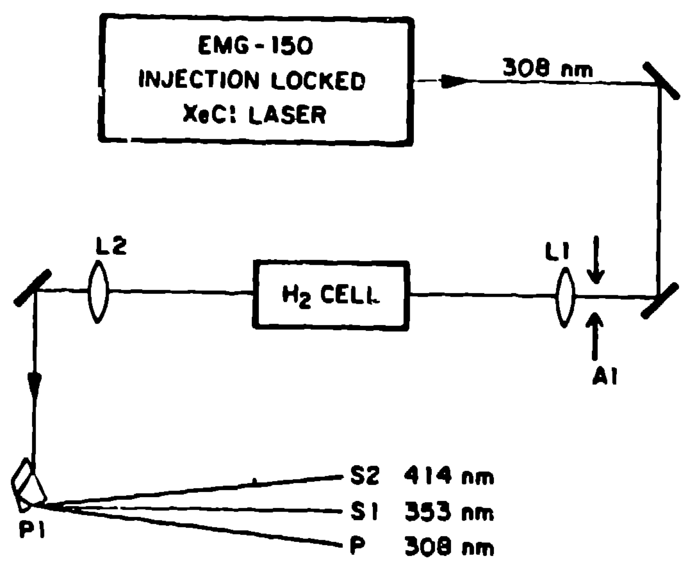

Fig. 1. Experimental Apparatus. The incident XeCl beam at 308 nm is clipped by aperture A1 and then focused with a 2-m lens L1 into a 50-cm cell containing typically 1500 psi of H_2. The prism P1 separates the pump P, first Stokes S1, and second Stokes S2 for energy and power measurements.

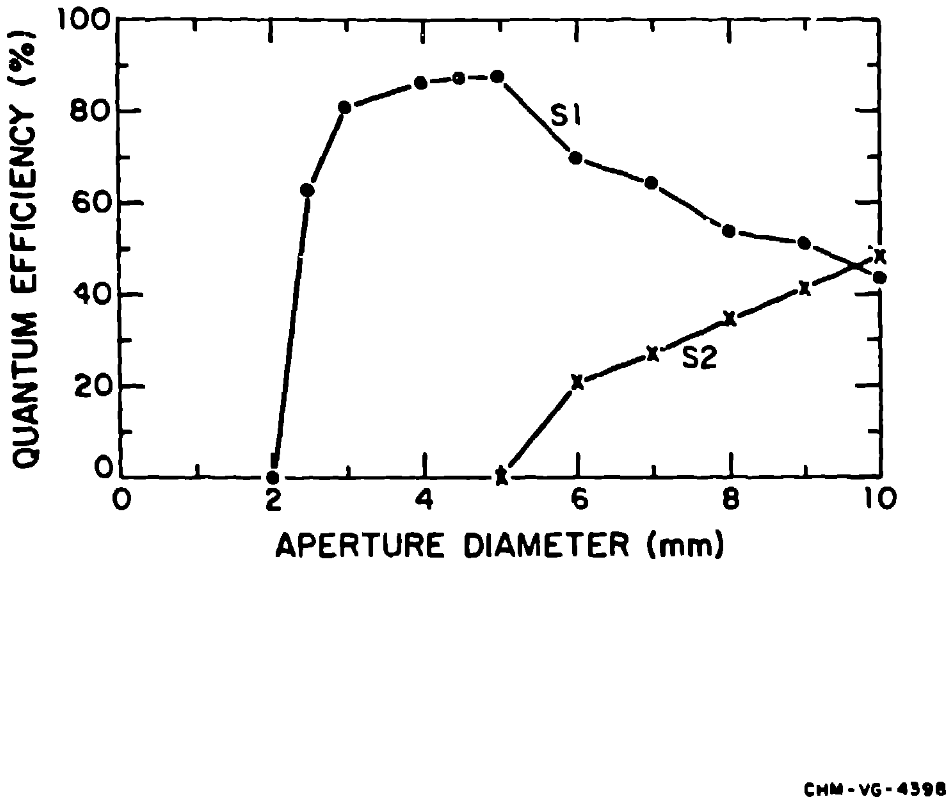

Fig. 2. Variation of quantum efficiency of first Stokes S1 and second Stokes S2 as a function of aperture diameter for an incident fluence of ~44 mJ/cm^2. S1 is seen to peak at 88% quantum efficiency before dropping as S2 increases at large aperture diameters.

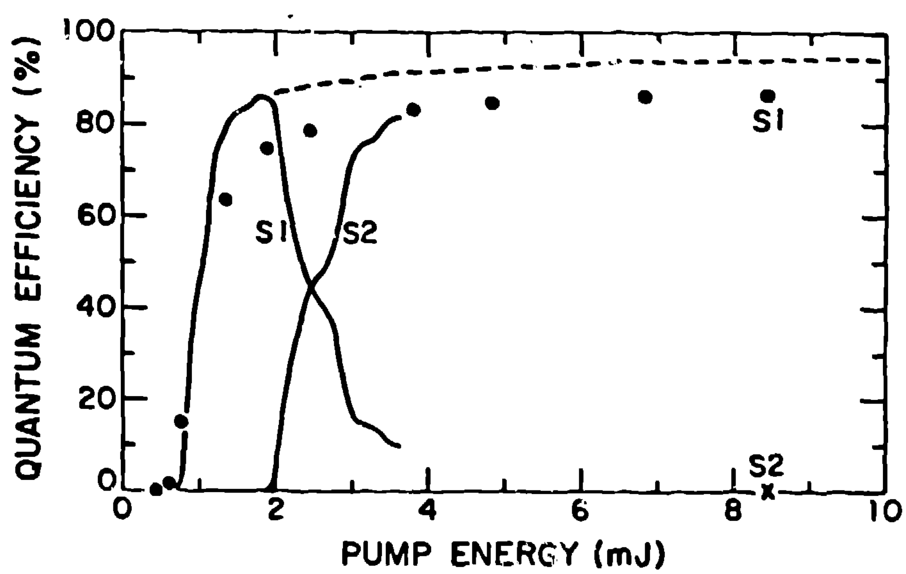

CHM-VG-4395

Fig. 3. Quantum efficiency of S1 and S2 as a function of incident pump energy with the aperture set to 4.5 mm diameter. The H_2 pressure in the cell was 1430 psi. The solid lines show the expected growth of S1 and S2 for a plane wave model using eqs. 1-3 and the temporal pulse shape shown in Fig. 4. The dashed line shows the growth of S1 if the gain for S2 is set arbitrarily to zero.

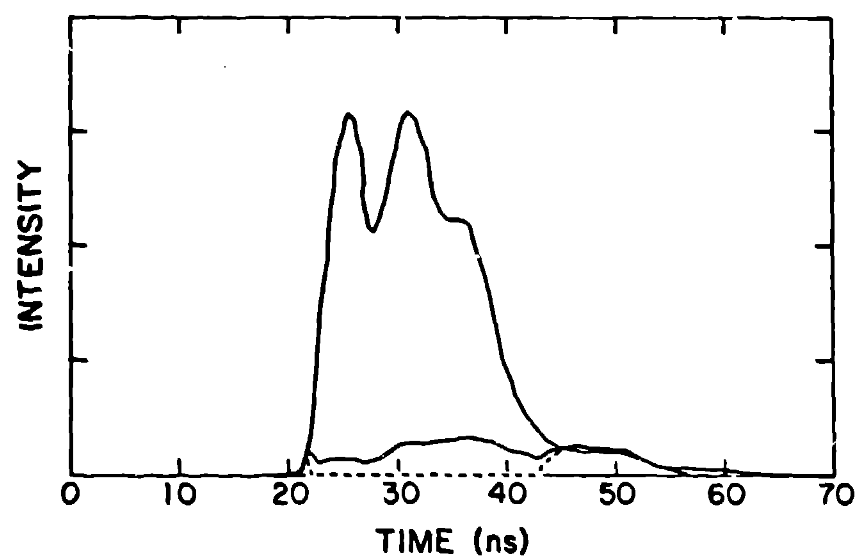

Fig. 4. Experimental pulse shape showing pump depletion for an aperture diameter of 4.5 mm and an incident pump energy of 6.5 mJ. Solid lines show the experimentally observed input pulse and output pulse. Dotted line shows the pump depletion predicted from eqs. 1-3.

References

1. N. Djeu and R. Burnham, "Efficient Raman conversion of XeF laser output in Ba vapor," Appl. Phys. Lett. 30, 473 (1977).

2. S. J. Brosnan, H. Komine, E. A. Stappaerts, M. J. Plummer, and J. B. West, "High-efficiency joule-level Raman generator in Pb vapor," Opt. Lett. 7, 154 (1982).

3. P. Rabinowitz, A. Stein, R. Brickman and A. Kaldor, "Efficient tunable H_2 Raman laser," Appl. Phys. Lett. 35, 739 (1979).

4. J. L. Carlsten and R. G. Wenzel, "Stimulated rotational Raman scattering in CO_2 - pumped para-H_2," IEEE J. Quant. QE-19, 1407 (1983).

5. T. R. Loree, R. C. Sze, and D. L. Barker, "Efficient Raman shifting of ArF and KrF laser wavelengths," Appl. Phys. Lett. 31, 37 (1977).

6. H. Komine and E. A. Stappaerts, "Efficient higher-Stokes-order Raman conversion in molecular gases," Opt. Lett. 4, 398 (1979).

7. I. V. Tomov, R. Fedosejevs, D. C. D. McKen, C. Domier, and A. A. Offenberger, "Phase conjugation and pulse compression of KrF - laser radiation by stimulated Raman scattering," Opt. Lett. 8, 9 (1983).

8. W. Kaiser and M. Maier, "Stimulated Rayleigh, Brillouin, and Raman spectroscopy," in Laser Handbook, F. T. Arecchi and E. O. Schulz-Dubois, eds. (North-Holland, Amsterdam, 1972), p. 1096.

9. Note that Ref.[8] indicates that the coeficient for the second term on the right side of equation (1) should be α_p. This is only true when the frequency dependence of the polarizability is negligible, so that $\alpha_p \propto \omega_{S1}$ and $\alpha_{S1} \propto \omega_{S2}$. According to Ref. [10] $\alpha_p \approx 6.8 \times 10^{-9}$ cm/w and $\alpha_{S1} = 5.4 \times 10^{-9}$ cm/w, which give $\alpha_{S1}(\omega_{S1}/\omega_{S2}) = 6.5 \times 10^{-9} \neq \alpha_p$. This is due to the resonant enhancement of the polarizability.

10. W. K. Bischel and G. Black, "Wavelength dependence of Raman scattering cross sections from 200-600 nm," in Excimer Lasers - 1983, C. K. Rhodes, Egger, and H. Pummer, eds. (Amer. Inst. Phys., New York, 1983) p. 101; corrections to the above paper by private communication with W. K. Bischel.

Figure Captions

Fig. 1. Experimental Apparatus. The incident XeCl beam at 308 nm is clipped by aperture A1 and then focused with a 2-m lens L1 into a 50-cm cell containing typically 1500 psi of H_2. The prism P1 separates the pump P, first Stokes S1, and second Stokes S2 for energy and power measurements.

Fig. 2. Variation of quantum efficiency of first Stokes S1 and second Stokes S2 as a function of aperture diameter for an incident fluence of ~44 mJ/cm^2. S1 is seen to peak at 88% quantum efficiency before dropping as S2 increases at large aperture diameters.

Fig. 3. Quantum efficiency of S1 and S2 as a function of incident pump energy with the aperture set to 4.5 mm diameter. The H_2 pressure in the cell was 1430 psi. The solid lines show the expected growth of S1 and S2 for a plane wave model using Eqs. (1)-(3) and the temporal pulse shape shown in Fig. 4. The dashed line shows the growth of S1 if the gain for S2 is set arbitrarily to zero.

Fig. 4. Experimental pulse shape showing pump depletion for an aperture diameter of 4.5 mm and an incident pump energy of 6.5 mJ. Solid lines show the experimentally observed input pulse and output pulse. Dotted line shows the pump depletion predicted from Eqs. (1)-(3).